ELSEVIER

Journal of Nuclear Materials 257 (1998) 256–262

journal of nuclear materials

Thermodynamic analysis of the Cs–Te system around the Cs_2Te phase

H.P. Nawada, O.M. Sreedharan *

Metallurgy Division, IGCAR, Kalpakkam, Tamil Nadu 603102, India

Received 7 June 1997; accepted 12 June 1998

Abstract

The temperature dependent and concentration asymmetric interaction parameter in the liquid phase region is computed from reliable thermodynamic data and phase-boundary composition by treating the single liquid phase of Cs–Te as a sub-regular solution. The excess Gibbs energy of the liquid phase of Cs–Te is determined to be $G_E^L = x_{Cs} \times x_{Te} \{(-289 - 0.00144 \times T)\, x_{Te} + (-972 + 0.482713 \times T)\, x_{Cs}\}$ kJ/mol in the temperature range 900–1100 K. The interaction parameter so deduced is used to calculate the activities of Te and Cs in the single liquid phase and two-phase regions around Cs_2Te.

PACS: 60–61.25Mv; 20–28.50Ft; 20–28.41Bm; 20–28.52Fa

1. Introduction

Since Te was found to be present in some of the inclusions [1,2] in the cladding alloys of irradiated fuel pins of LMFBRs, there were quite a few investigations in the literature on different aspects of fuel-cladding chemical interactions (FCCI). The equilibrium calculations made by Cordfunke and Konings [3] and Imoto and Tanabe [4] had shown that the predominant tellurium bearing species in an operating fuel rod was Cs_2Te. PIE has shown that the oxygen partial pressure plays an important role on the Cs, Te – cladding interaction. Caesium, tellurium and their compounds cause corrosion of the cladding alloys in LMFBRs. Decomposition of Cs_2Te due to either increase in temperature or reaction with other fission products could lead to the release of more Te thereby resulting in clad attack. This process of clad attack by Cs and Te was investigated in a very systematic manner by Pulham and his coworkers [5] under varying conditions of the Cs/Te ratio and local oxygen potentials. Recently, the Cs-rich part of the Cs–Te phase diagram was revised by de Boer and Cordfunke [6]. Subsequently a critical review of all available data on the Cs–Te phase diagram was published by Okamoto [7]. There are no direct experimental measurements on the activity of Te in the Cs–Te system as well as on the phase boundary data on the Cs-rich side of Cs_2Te (s) + liquid, L. The activity of Te in the binary Cs–Te system in the high temperature region namely, 900–1100 K as a function of composition and also knowledge of the Cs-rich phase boundary of Cs_2Te (s) + L which determines the invariant Te potential field would be of immense help in evaluating the clad stability with respect to Te [8]. Hence, an attempt is made in this paper to elucidate necessary thermodynamic data for the Cs–Te system from the available experimentally determined phase diagram information [6,9–11], Gibbs energies of formation of Cs_2Te (s) [12], Cs_5Te_3(s) [13] and enthalpy of fusion of Cs_2Te (s) [6] as well as pure Te [14].

2. Methodology

The liquid region of Cs–Te is considered as a non-ideal solution and the Gibbs energy of the liquid L is given by

---

* Corresponding author. Tel.: +91-4114 40202; fax: +91-4114 7360; e-mail: oms@igcar.ernet.in.

0022-3115/98/$ – see front matter © 1998 Elsevier Science B.V. All rights reserved.
PII: S 0 0 2 2 - 3 1 1 5 (9 8) 0 0 4 5 8 - 9

$$G^{\mathrm{L}} = x_{\mathrm{Cs}} \times G^{\mathrm{L}}_{\mathrm{Cs}} + x_{\mathrm{Te}} \times G^{\mathrm{L}}_{\mathrm{Te}} + R \times T\,\{x_{\mathrm{Cs}} \times \ln(x_{\mathrm{Cs}}) + x_{\mathrm{Te}} \times \ln(x_{\mathrm{Te}})\} + G^{\mathrm{L}}_{\mathrm{E}}, \tag{1}$$

where x_{Cs} and x_{Te} are the atom fractions in the liquid phase, $G^{\mathrm{L}}_{\mathrm{Cs}}$ and $G^{\mathrm{L}}_{\mathrm{Te}}$ are the Gibbs energies in the liquid phase, and the excess Gibbs energy $G^{\mathrm{L}}_{\mathrm{E}}$ is a function of temperature and composition. Various solution models such as ideal, regular, sub-regular [15], ideal associated solution [16] as well as various polynomial expression based models such as Pelton's orthogonal polynomial [17], Lupis [18], Margules [19], Hazra [20] and Gokcen [21] were also tested to arriving at the sub-regular solution approach. The selection of the best fitting model among these models was based on its predictability of (i) phase transition points, (ii) phase boundaries (iii) Gibbs energy formation of compound phases and (iv) reasonable Te and Cs potentials. For a sub-regular solution approach, the excess Gibbs energy $G^{\mathrm{L}}_{\mathrm{E}}$ could take the form

$$G^{\mathrm{L}}_{\mathrm{E}} = x_{\mathrm{Cs}} \times x_{\mathrm{Te}} \times \{(R_1 + R_2 \times T) \times x_{\mathrm{Cs}} + (S_1 + S_2 \times T) \times x_{\mathrm{Te}}\}. \tag{2}$$

One could compute chemical potentials [15] of Cs and Te by differentiating Eq. (1) with the number of moles of Te or Cs, and by equating the chemical potentials of Cs and Te at the phase boundary with those of Cs_2Te (s) + L/L, the following equation was derived:

$$\Delta_{\mathrm{f}} G^0(\mathrm{Cs_2Te, s})/3 - R \times T/3\,[\ln(x_{\mathrm{Te}}) + 2 \times \ln(1 - x_{\mathrm{Te}})] - (R_1 + R_2 \times T)/3\,[6x^3_{\mathrm{Te}} - 3x^2_{\mathrm{Te}} + 2x_{\mathrm{Te}}] - (S_1 + S_2 \times T)/3\,[1 - 4x_{\mathrm{Te}} + 9x^2_{\mathrm{Te}} - 6x^3_{\mathrm{Te}}] = 0, \tag{3}$$

where $\Delta_{\mathrm{f}} G^0$ (Cs_2Te, s) is the Gibbs energy of formation per mole of Cs_2Te. However, it is assumed that the compound phases under consideration are perfectly stoichiometric. In a similar way, by equating the chemical potential of Cs and Te at the phase boundary with those of Cs_5Te_3 (s) + L/L, the following equation was derived:

$$\Delta_{\mathrm{f}} G^0(\mathrm{Cs_5Te_3, s})/8 - RT/8\,[3 \times \ln(x_{\mathrm{Te}}) + 5 \times \ln(1 - x_{\mathrm{Te}})] - (R_1 + R_2 \times T)/8\,[6 \times x^2_{\mathrm{Cs}} \times x_{\mathrm{Te}} + 5 \times x^2_{\mathrm{Te}}\,(1 - 2 \times x_{\mathrm{Cs}})] - (S_1 + S_2 \times T)/8\,[x^2_{\mathrm{Cs}} \times (3 - 6x_{\mathrm{Te}}) + 10 \times x^2_{\mathrm{Te}} \times x_{\mathrm{Cs}}] = 0. \tag{4}$$

Similarly by equating the Te potential with that at Te (s) + L/L phase boundary one would obtain

$$\Delta G^{\mathrm{Te(s)} \to \mathrm{L}} + RT \times [\ln(1 - x_{\mathrm{Te}})] + 2 \times (R_1 + R_2 \times T) \times (x^3_{\mathrm{Te}} - 2x^2_{\mathrm{Te}} + x_{\mathrm{Te}}) - (S_1 + S_2 \times T)(1 - 4x_{\mathrm{Te}} + 5x^2_{\mathrm{Te}} - 2x^3_{\mathrm{Te}}) = 0. \tag{5}$$

The experimental measurements of the phase boundaries on the Te-rich side of Cs_2Te(s) were from de Boer and Cordfunke [6], Drowart [9] as well as Chuntonov et al. [10]. Data on the Gibbs energy of formation of (Cs_2Te, s) were taken from the handbook on reactor materials by Cordfunke and Konings [12]. These values were polynomilized for interpolation purpose in the temperature range of interest namely 900–1100 K.

$$\Delta_{\mathrm{f}} G^0(\mathrm{Cs_2Te, s}) = c_1 + c_2 \times T + c_3 \times T^2 + c_4/T \text{ kJ/mol}. \tag{6}$$

The values were $c_1 = -215.681$; $c_2 = -0.25791$; $c_3 = 1.981346 \times 10^{-4}$ and $c_4 = -23045.1$, respectively. Similarly, the recent data by de Boer and Cordfunke [13] on the Gibbs energy of formation of Cs_5Te_3 (s) were also polynomilized into the following equational form in the temperature range of 720–930 K:

$$\Delta_{\mathrm{f}} G^0(\mathrm{Cs_5Te_3, s}) = d_1 + d_2 \times T + d_3 \times T^2 + d_4/T + d_5 \times \log T \text{ kJ/mol}. \tag{7}$$

The values were $d_1 = -2645.26$; $d_2 = -0.67395$; $d_3 = 3.43784 \times 10^{-4}$; $d_4 = 38703.15$ and $d_5 = 715.922$, respectively. The experimental data on the phase boundary of Te (s) + L/L were taken from Chuntonov et al. [10] and Adamson and Leighty [11]. Data on the Gibbs energy difference between pure solid Te (fcc) and liquid Te was taken from Knacke et al. [14]. The interaction parameters in the liquid phase were estimated by linear regression of Eqs. (3)–(5). The optimum excess Gibbs energy terms of liquid Cs–Te obtained by regression (see Eq. (2)) were $R_1 = -289$ kJ/mol; $R_2 = -0.00144$ kJ/mol; $S_1 = -972$ kJ/mol and $S_2 = 0.482713$ kJ/mol.

These excess solution parameters were utilized to compute the liquidus points around Cs_2Te (s) and Cs_5Te_3 (s) by solving Eq. (3) and Eq. (4) for x_{Te}.

3. Results and discussion

The computed liquidus on the Te-rich side is reasonably in close agreement (see Fig. 1) with the recently assessed phase-boundary by Okamoto [7]. However, the computed liquidus on the Cs-rich side differs significantly from the one predicted by Okamoto. The present model predicts a symmetric liquidus around Cs_2Te while that shown by Okamoto is a rather asymmetric liquidus around Cs_2Te. In order to make a more accurate representation of the phase boundaries around Cs_2Te, the following factors should be taken into account:

(a) The considerable non-stoichiometric range around $Cs_{2-x}Te$

(b) The possible effect of transition from α to β phase on the stoichiometry could give rise to one of the four possible overlapping reaction pathways namely

(i) Solid solutions of α and β of Cs_2Te flanked in between by a two-phase field of α and β

(ii) Peritectic formation of α-phase (namely L + β → α) occurring at a slightly higher temperature than the α → β transition temperature.

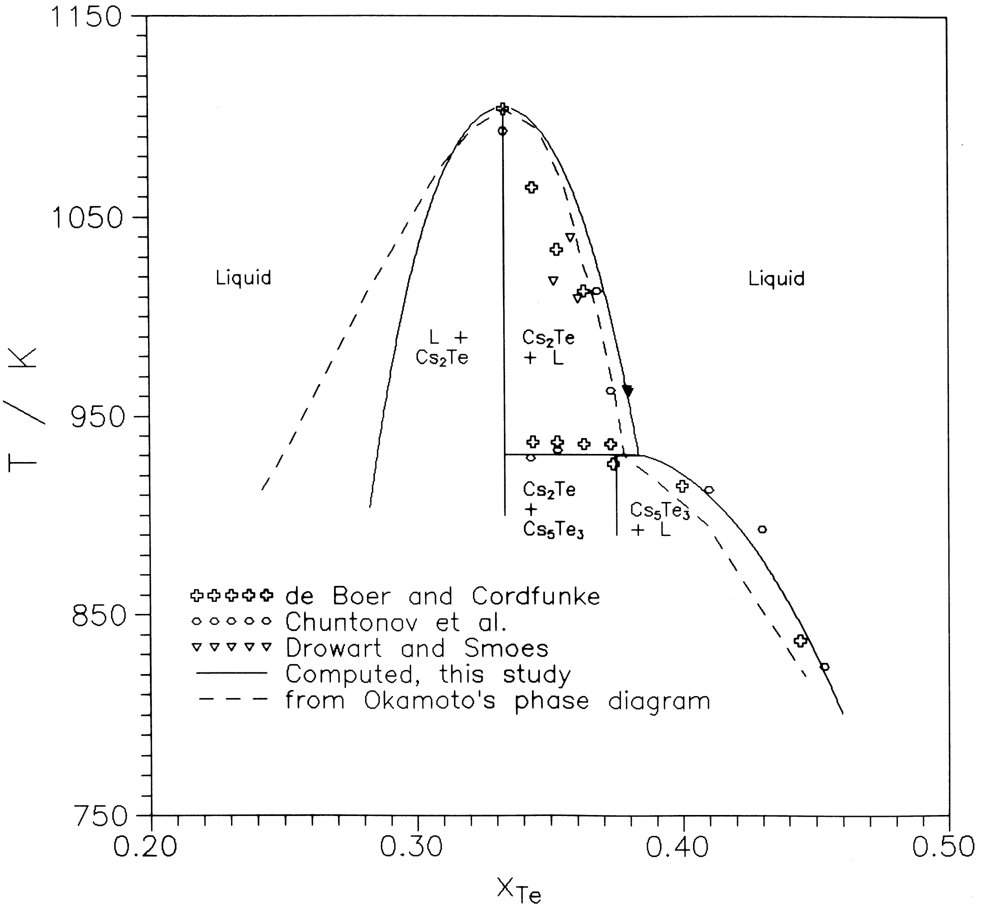

Fig. 1. Comparison of calculated liquidus points around Cs_2Te in the Cs–Te binary system using the sub-regular solution model (this work) with the experimental data points [6,9,10] and assessed phase diagram [7].

(iii) Formation by a peritectoid reaction $\beta + Cs_5Te_3 \rightarrow \alpha$ occurring at a slightly higher temperature than the α–β transition temperature.

(iv) A metatectic decomposition of the β-phase like $\beta \rightarrow L + \alpha$ which could happen just before the $\alpha \rightarrow \beta$ transition reaction.

Since information on the stoichiometric range of $Cs_{2-x}Te$ is insufficient to be taken into account and the existing information in the literature does not permit identification of the reaction pathway, it is deemed that the symmetric liquidus representation around the congruently melting Cs_2Te is a more acceptable representation than what has been suggested by Okamoto.

It is clearly evident that from the liquidus region around Cs_2Te (s) (see Fig. 1) the two-phase region Cs_2Te (s) + L is found to spread from 0.2877 to 0.3333 only on the Cs-rich side while on the Te-rich side, it extends 0.3333 to the maximum of 0.381. Te potential for the liquid single-phase region of Cs–Te was computed as a function of the Te mole fraction utilizing the excess Gibbs energy terms

$$\overline{\Delta G}_{Te} = RT \times \ln(x_{Te}) + x_{Cs}^2\,[2 \times x_{Te}(R_1 + R_2 \times T) + (S_1 + S_2 \times T)\,(1 - 2 \times x_{Te})] \qquad (8)$$

and results are presented in Fig. 2. The computed Te potential at 1000 K is found to increase monotonically from −326.2 to −194.3 kJ/mol with increasing Te mole fraction from 0.150 to 0.296, while the Cs potential decreases from −15.5 to −52.9 kJ/mol in the same concentration region. On further addition of Te to the single-phase liquid results in precipitation of Cs_2Te (s). Since the two-phase region would have an invariant potential for a fixed temperature, both Te and Cs potentials would remain constant at −194.3 and −52.9 kJ/mol, respectively until the Te mole fraction reaches 0.333. Addition of Te beyond the composition of 0.333 should lead to the formation of a single-phase line compound Cs_2Te (s). Upon further increment of Te to this composition results in appearance of the two phase mixture namely Cs_2Te (s) with liquid which is rich in Te thus forcing both the Te and Cs potentials jump sharply to the new constant values namely −142.9 and −78.6 kJ/

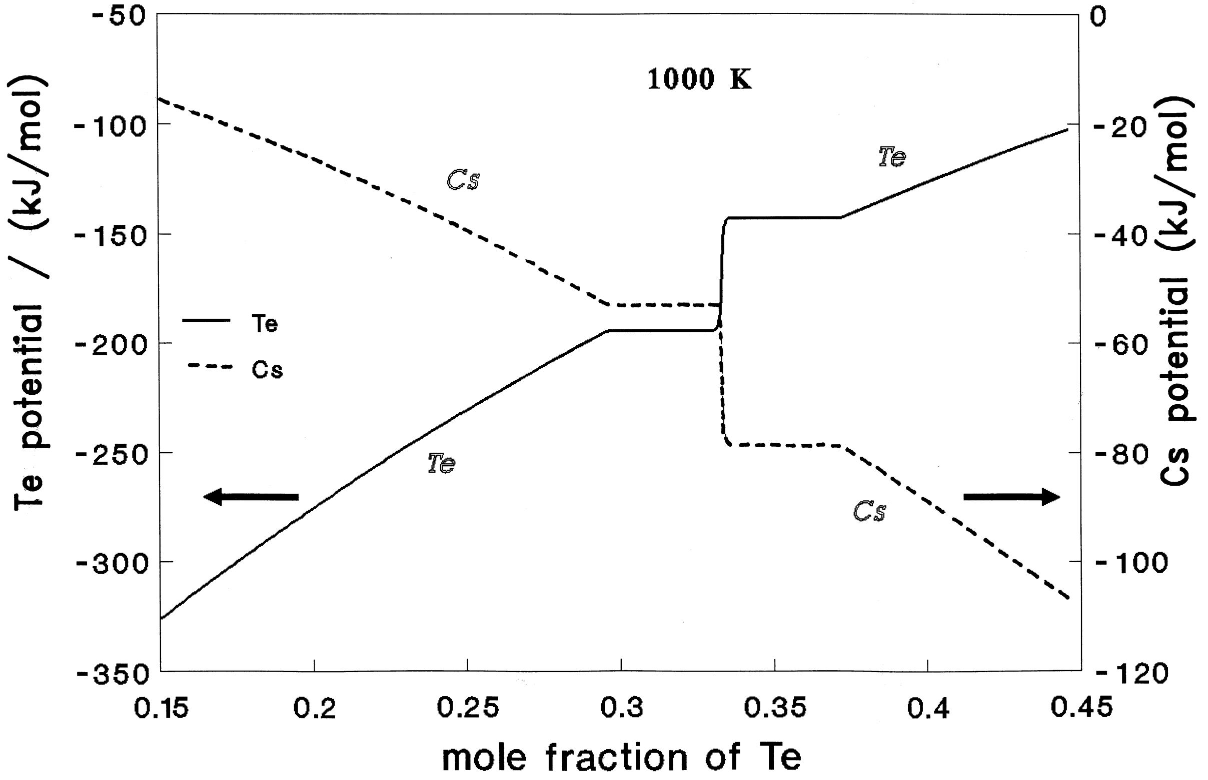

Fig. 2. Illustration of variation of calculated chemical potentials of Te and Cs for the Cs–Te system at 1000 K as a function of Te mole fraction.

mol, respectively. These constant chemical potential fields would prevail up to the phase boundary namely that of Cs_2Te + L with L. Incidentally, Drowart and Smoes [9] and Portman et al. [22] have measured the partial pressure of various Cs and Te vapour species in the temperature range 850–1320 K. However, there are some uncertainties in the initial compositions and oxygen impurities in their measurements. Measurements of Drowart and Smoes were more extensive (namely roughly 200 experimental observations) covering a wide temperature range and in addition to the initial composition were close to Cs_2Te. Chemical potentials of Te and also Cs were calculated from their vapour pressure data [9] and together with the knowledge of those for vapour pressure data of pure elements for standard reference states namely pure solid or liquid [14]. Te potentials could be calculated indirectly by computing the decomposition constant for the gas phase reaction $(CsTe)_{gas} \leftrightarrow (Cs)_{gas} + (Te)_{gas}$ in conjuction with the partial pressure of $(CsTe)_{gas}$ and $(Cs)_{gas}$. Drowart and Smoes had reported only partial pressure of $(Cs)_{gas}$ and $(CsTe)_{gas}$ in the majority of their work. However, in one experiment (Exp 3. of Ref. [9]) they have reported all the three species namely $(CsTe)_{gas}$, $(Cs)_{gas}$ and $(Te)_{gas}$ in the temperature range from 1153 to 1322 K. In this temperature region the decomposition constant for the gas phase decomposition of $(CsTe)_{gas}$ to $(Cs)_{gas}$ and $(Te)_{gas}$ was computed. The partial pressure of Te was calculated by extrapolating/interpolating the decomposition behaviour of $(CsTe)_{gas}$ for the temperature range of 850–1320 K together with the knowledge of the partial pressures of $(CsTe)_{gas}$ and $(Cs)_{gas}$. These Te potentials were found to scatter over a span of −65 to −90 kJ/mol corresponding to the variation of the temperature from 820 to 1320 K. According to these authors, at very high temperature, viz., above 1100 K, the composition of the initial sample around Cs_2Te would steadily get enriched with Te owing to the incongruent vaporization behaviour of the Cs–Te alloys. These Te and Cs potential values were fitted to an approximate linear relation ignoring the effect of compositional variation among the samples on chemical potential

$$\overline{\Delta G_{Te}} = -34.5072 - 0.0421358 \times T \text{ (kJ/mol)}, \qquad (9)$$

$$\overline{\Delta G_{Cs}} = -168.247 + 0.056757 \times T \text{ (kJ/mol)}. \qquad (10)$$

The values of the Cs potentials were linearized only in the temperature range 850–1100 K. Because at temperatures above 1100 K the Cs potentials were found to be abnormally low besides exhibiting a reverse trend in their values with respect to temperature. Using the excess Gibbs energy terms derived from the present model, the Te and Cs potentials for both the phase boundaries namely Cs_2Te (s) + L coexisting with L as a function of temperature were computed. The model-predicted values of Te and Cs potentials were significantly different from the computed ones from those of experimental values of Drowart and Smoes (Figs. 3 and 4). The model-predicted Te potential values for the Te-rich liquidus were found to vary from −160 to −138 kJ/mol for the temperature variation of 1100–930 K while the corresponding experimental Te potential values were approximately in the range of −80.9 to −73.7 kJ/mol. Incidently, the model predicted Cs potentials for the above mentioned phase field were −59 to −89 kJ/mol while the corresponding experimental values were −105.8 to −115.5 kJ/mol. As per the model, to attain such a high negative chemical potential the Te mole fraction would be roughly above 0.48 which happens to be the single-phase liquid in the temperature range of interest. Regardless of preferential evaporation of Cs at higher temperature it was most unlikely that the initial composition of 0.333 (Te mole fraction) could drift to 0.48. Nevertheless, the large discrepancy could be attributed (i) to the assumption made in the present model (viz., assuming the compound phase Cs_2Te to be perfectly stoichiometric) and (ii) the possible role of trace level oxygen present in the sample. Further, the propensity of Cs to react with oxygen in conjunction with the negligible solubility of oxygen in liquid Te would manifest in the lowering of the Cs potential drastically and simultaneous increase of the Te potential. Perhaps, this could be the reason for the large difference between the experimental values and those predicted by the model. The role of oxygen would be examined in a future independent investigation on the ternary Cs–Te–O system. Nonetheless, the compositions of the majority of the low temperature (900–1100 K) Te potential values of Drowart and Smoes were found to be in the vicinity of the Te-rich liquidus of Cs_2Te. On the contrary, the corresponding Te partial pressures for the Cs-rich phase

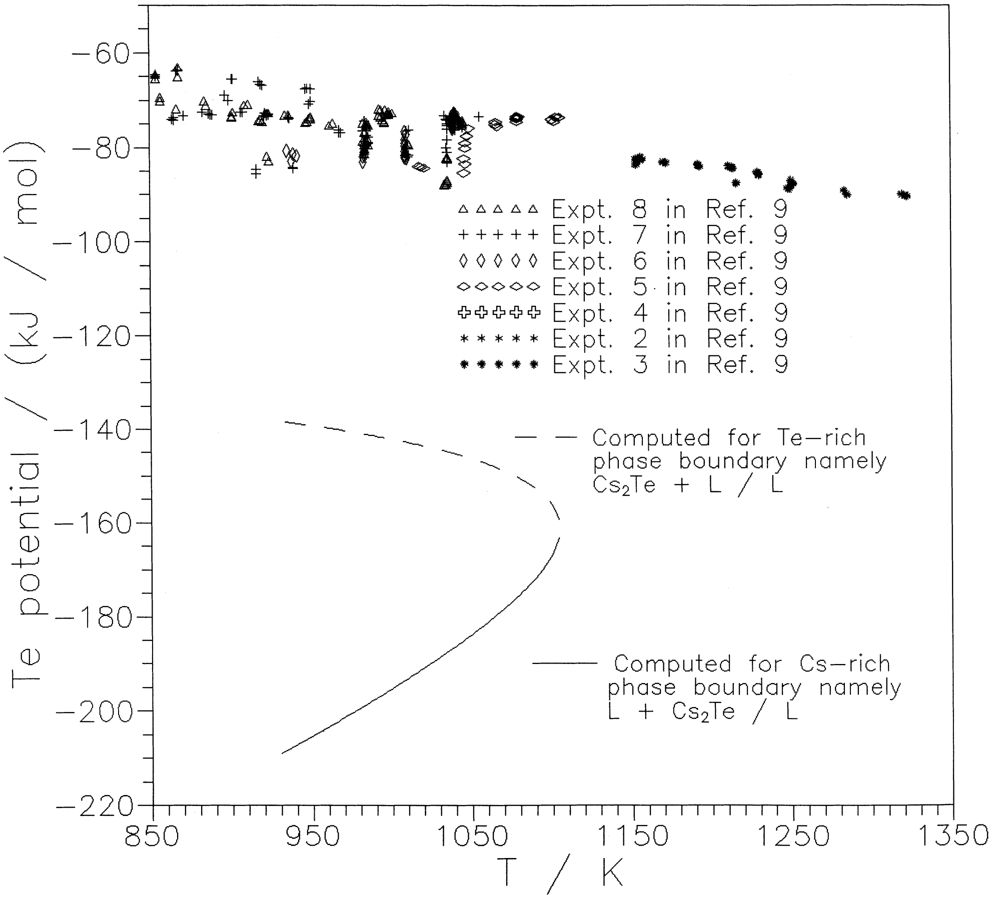

Fig. 3. Comparison of Te potentials predicted by the model with those computed from the data of Drowart and Smoes [9] for the two phase regions approaching Cs_2Te (s).

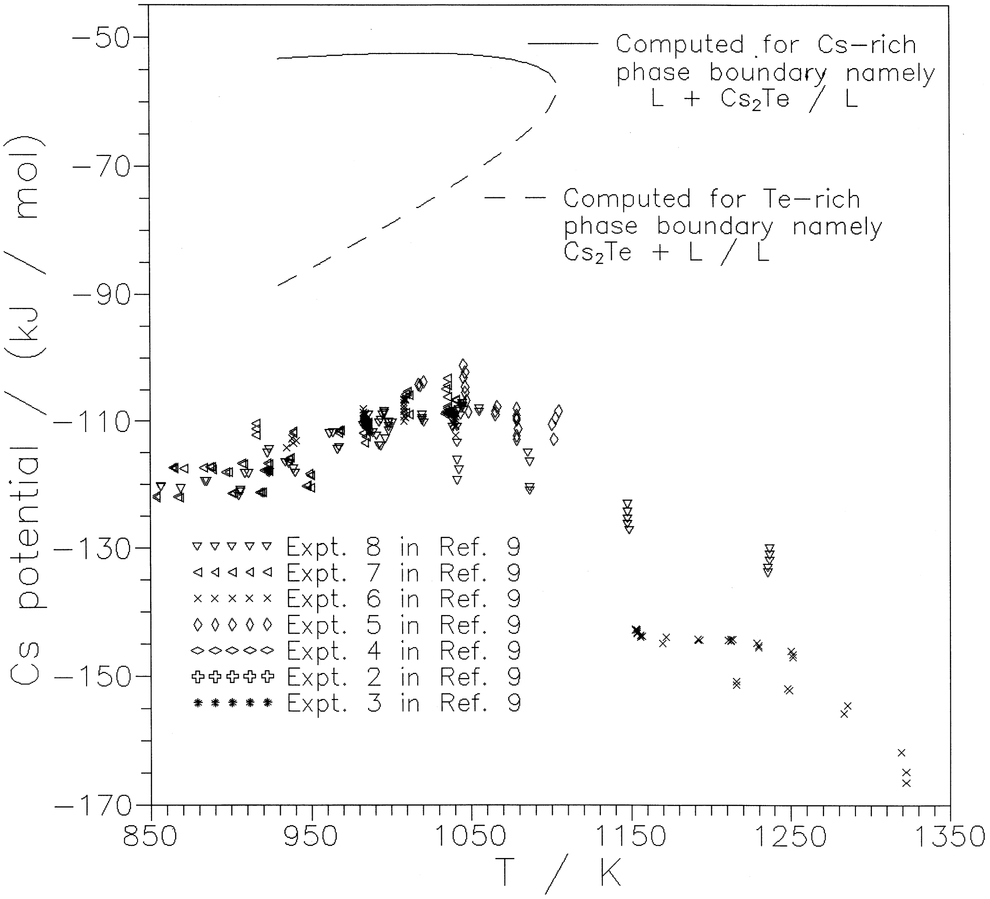

Fig. 4. Comparison of Cs potentials predicted by the model with those computed from the data of Drowart and Smoes [9] for the two phase regions approaching Cs_2Te (s).

boundary (i.e., $\langle Cs_2Te\rangle$ + L) would be few orders of magnitude lower (perhaps may be more negative than −110 kJ/mol in terms of Te potentials) than those for the Te-rich liquidus boundary; this should be attributable to the steep rise caused by the sudden change over in composition into the other biphasic field (depiction similar to Fig. 2).

The adjoining phase of Cs_2Te (s) is Cs_5Te_3 (s) and this phase coexists with liquid from 930 to 720 K. The liquidus points of de Boer and Cordfunke [6] were taken for computation. Although Chuntonov et al. [10] had identified solid compounds different from those by compared to de Boer and Cordfunke, still their liquidus was found to be close to that by the later investigators [6]. The standard Gibbs energy of formation of Cs_5Te_3 (s) was computed by calculating the Te and Cs potentials with the aid of the excess Gibbs energy terms at the phase boundary of Cs_5Te_3 + L with L is as given below.

$$\Delta_f G^0(Cs_5Te_3(s)) = 3 \times \overline{\Delta G}_{Te} + 5 \times \overline{\Delta G}_{Cs}. \quad (11)$$

The values $\Delta_f G^0(Cs_5Te_3(s))$ by use of above (Eq. (11)) and upon linear regression yielded

$$\Delta_f G^0(Cs_5Te_3, s) = -1550.32 + 0.743852 \times T \text{ kJ/mol.} \quad (12)$$

The predicted Gibbs energy of formation of Cs_5Te_3 from the model was comparatively more negative than the recent experimental Gibbs energy data of de Boer and Cordfunke [13].

In a similar manner, the Gibbs energy of formation of CsTe(s) (caesium monotelluride) could not be calculated from the experimental results on CsTe (s) + L/L owing to the limited number of data points namely just three, out of which two points were for the same temperature. Likewise, the Gibbs energy of formation of Cs_2Te_3 (s) which is another phase that coexists with liquid in the temperature range 530–660 K was calculated using an identical approach described earlier,

$$\Delta_f G^0(Cs_2Te_3, s) = -777.829 + 0.356435 \times T \text{ kJ/mol.} \quad (13)$$

The prediction of the Gibbs energies of formation of intermetallic phases in binary systems typically involves the assumption that the liquidus or solvus compositions in equilibrium with the phase were correct and extrapolation of the solution model to a wider composition and temperature range would be reasonable. In addition to these uncertainties, the non-stoichiometry in the intermediate compound phase would also alter the prediction.

Tellurium potential of this liquid alloy of Cs–Te together with traces of oxygen that could get dissolved in it due to the imposition of the local oxygen potential would determine whether the clad components would react to form tellurides. In this context, the present work illustrates the first part of our understanding namely the role of the Cs–Te system in fixing the Te potential in FCCI problems. Complete visualization of Te reactions with clad would be possible only when the Cs–Te–O ternary were comprehensively established.

4. Conclusions

1. Among various solution models the sub-regular solution approach was found to give an optimum thermodynamic representation of the liquid phase of the Cs–Te system. The excess Gibbs energy of the liquid phase of Cs–Te could be represented as (in kJ/mol)

$$G_{\mathrm{E}}^{1} = x_{\mathrm{Cs}} \times x_{\mathrm{Te}} \{(-289 - 0.00144 \times T)\, x_{\mathrm{Te}} + (-972 + 0.482713 \times T)\, x_{\mathrm{Cs}}\}.$$

2. The chemical potentials of Te and Cs in the liquid single-phase Cs–Te system could be derived as (in kJ/mol)

$$\overline{\Delta G}_{\mathrm{Te}} = R \times T \times \ln(x_{\mathrm{Te}}) + x_{\mathrm{Cs}}^{2}\, [2 \times x_{\mathrm{Te}}\, (R_1 + R_2 \times T) + (S_1 + S_2 \times T)\, (1 - 2 \times x_{\mathrm{Te}})],$$

$$\overline{\Delta G}_{\mathrm{Cs}} = R \times T \times \ln(x_{\mathrm{Cs}}) + x_{\mathrm{Te}}^{2}\, [(1 - 2 \times x_{\mathrm{Cs}})\, (R_1 + R_2 \times T) + (S_1 + S_2 \times T)^{2}\, x_{\mathrm{Cs}}].$$

3. The chemical potentials of Te and Cs computed from the vapour pressure measurements of Drowart and Smoes are significantly more positive compared to those of the model predictions. These differences could be due to the non-stoichiometry of Cs_2Te and the role of oxygen that could be present in the samples.

Acknowledgements

The authors are grateful to Dr Baldev Raj, Director Materials and Metallurgy Group and Dr V.S. Raghunathan, Head, Metallurgy Division for their keen interest and constant encouragement throughout the course of this work. This work reported here will form a part of the PhD thesis to be submitted to the University of Madras by the one of the authors, H.P.N.

References

[1] R.F. Hilbert, K.J. Perry, W.K. Appleby, W.E. Baily, C.N. Craig, General Electric Report, GEAP – 13538, 1973.
[2] H. Kleykamp, J. Nucl. Mater. 131 (1985) 221.
[3] E.H. P Cordfunke, R.J.M. Konings, J. Nucl. Mater. 201 (1993) 57.
[4] S. Imoto, T. Tanabe, J. Nucl. Mater. 154 (1988) 62.
[5] R.J. Pulham, M.W. Richards, J. Nucl. Mater. 171 (1990) 319.
[6] R. de Boer, E.H.P. Cordfunke, J. Alloys Compounds 228 (1995) 75.
[7] H. Okamoto, J. Phase Equil. 17 (1996) 550.
[8] H.P. Nawada, O.M. Sreedharan, Thermodynamic analysis of Cs–Te binary phase diagram, Proceedings of the International Conference on Biological and Chemical Thermodynamics, 5–8 January 1997, Guru Nanak Dev University, Amritsar, India, Paper 5A.
[9] J. Drowart, S. Smoes, Thermodynamic study of the Cs–Te, In–Te and Cs–In–Te systems with the mass spectrometric Knudsen cell method, Part B, in: R.G.J. Ball, S. Dickinson, E.H.P. Cordfunke, R.J.M. Konings, J. Drowart, S. Smoes (Eds.), Thermochemical Data Acquisition – Part III, Joint Final Report EUR 14844 EN, Commission of the European Communities, Luxembourg, Italy, 1992.
[10] K.A. Chuntonov, A.N. Kuznetsov, V.M. Fedorov, S.P. Yatsenko, Inorg. Mater. 18 (1982) 937.
[11] M.G. Adamson, J.E. Leighty, J. Nucl. Mater. 114 (1983) 327.
[12] E.H.P. Cordfunke, R.J.M. Konings, Thermochemical Data for Reactor Materials and Fission Products, North-Holland, Amsterdam, 1990.
[13] R. de Boer, E.H.P. Cordfunke, J. Chem. Thermodynamics 29 (1997) 603.
[14] O. Knacke, O. Kubaschewski, K. Hesselmann, Thermochemical Properties of Inorganic Substances, Springer, Berlin, 1991.
[15] L. Kaufman, H. Bernstein, Computer Calculation of Phase Diagrams, Academic Press, New York, 1970, p. 37.
[16] A.S. Jordan, Metall. Trans. 1 (1970) 239.
[17] C.W. Bale, A.D. Pelton, Metall. Trans. 5 (1974) 2323.
[18] C.H.P. Lupis, Chemical Thermodynamics of Materials, North-Holland, Amsterdam, 1983, p. 176.
[19] E. Hala, J. Pick, V. Fried, O. Vilim, Vapour–Liquid Equilibrium, 2nd ed., Pergamon, New York, 1967 (translated by G. Standart).
[20] J.P. Hazra, Metall. Trans. B. 11B (1990) 215.
[21] N.A. Gokcen, Thermodynamics, Techscience Inc., Hawthorne, CA, 1975.
[22] R. Portman, M.J. Quinn, N.H. Sarget, P.P.S. Saluja, D.J. Wern, Thermochim. Acta 144 (1989) 21.